Shallow BF_2 implants in Xe-bombardment-preamorphized Si: The interaction between Xe and F

M. Werner, J. A. van den Berg,[a] D. G. Armour, and G. Carter
Joule Physics Laboratory, Institute of Materials Research, University of Salford, Salford, M5 4WT, United Kingdom

T. Feudel and M. Herden
AMD Saxony LLC & Co. KG, Wilschdorfer Landstrasse 101, D-01109 Dresden, Germany

M. Bersani and D. Giubertoni
ITC-IRST, 38050 Povo-Trento, Italy

L. Ottaviano, C. Bongiorno, and G. Mannino
CNR-IMM, 95121 Catania, Italy

P. Bailey and T. C. Q. Noakes
CCLRC Daresbury Laboratory, Daresbury, WA4 4A, United Kingdom

(Received 7 December 2004; accepted 8 March 2005; published online 5 April 2005)

Si(100) samples, preamorphized to a depth of ~30 nm using 20 keV Xe ions to a nominal fluence of 2×10^{14} cm^{-2} were implanted with 1 and 3 keV BF_2 ions to fluences of 7×10^{14} cm^{-2}. Following annealing over a range of temperatures (from 600 to 1130 °C) and times the implant redistribution was investigated using medium-energy ion scattering (MEIS), secondary ion mass spectrometry (SIMS), and energy filtered transmission electron microscopy (EFTEM). MEIS studies showed that for all annealing conditions leading to solid phase epitaxial regrowth, approximately half of the Xe had accumulated at depths of 7 nm for the 1 keV and at 13 nm for the 3 keV BF_2 implant. These depths correspond to the end of range of the B and F within the amorphous Si. SIMS showed that in the preamorphized samples, approximately 10% of the F migrates into the bulk and is trapped at the same depths in a ~1:1 ratio to Xe. These observations indicate an interaction between the Xe and F implants and a damage structure that becomes a trapping site. A small fraction of the implanted B is also trapped at this depth. EXTEM micrographs suggest the development of Xe agglomerates at the depths determined by MEIS. The effect is interpreted in terms of the formation of a volume defect structure within the amorphized Si, leading to F stabilized Xe agglomerates or XeF precipitates. © *2005 American Institute of Physics*. [DOI: 10.1063/1.1900305]

B-doped source/drain and extension regions in Si complementary metal-oxide semiconductor devices are often produced using BF_2 ions for reasons of higher beam and hence wafer throughput. The behavior and effects of the implanted F has been widely studied.[1–11] Upon annealing F becomes mobile above 550 °C and is swept in front of the solid phase epitaxially regrown (SPER) layer, outward to the surface. A small fraction of the F migrates deeper in and is gettered at low concentration at defects beyond the original a/c interface.[4,8] At high BF_2 doses, F bubble formation may occur upon annealing and during SPER bubbles are swept ahead of the advancing interface. Bubble size increases for higher anneal temperatures.[9,10] At lower implant BF_2 doses (5×10^{14} cm^{-2}) that still result in amorphization, bubble formation was not seen but some F trapping at the end-of-range defects occurred.[6] For low fluence, non-amorphizing BF_2^+ implants only migration toward the surface and out diffusion is observed.[2] Although its behavior in Si is highly influenced by the defect structure, F chemistry also plays a strong role as, e.g., B enhanced diffusion is found to be retarded.[3,7]

Previous studies of inert gas ion implantation into Si and metals and annealing have shown that implanted ions tend to agglomerate or form bubbles depending on the implant dose.[12–15] In particular Xe has been shown to form bubbles in Si during annealing.[12]

Although BF_2 implantation is capable of amorphizing the Si matrix, deeper preamorphizing implants (PAI), using higher mass ions such as Ge, are preferred since they suppress channelling effects and enable the spatial separation of the end-of-range (EOR) defects and the junction depth. Heavier inert gas ions such as Xe form an attractive alternative to Ge because of the formation of sharper a/c interfaces. This article reports on the interaction of Xe from the PAI and F and B from the S/D BF_2^+ implants.

Implants of 1 and 3 keV BF_2^+ ions to a dose of 7×10^{14} cm^{-2} were carried out at room temperature into preamorphized and, for comparison, crystalline Cz, *p*-type Si(100). Cross-section transmission electron microscopy showed that the 20 keV Xe PAI to a dose of 2×10^{14} cm^{-2} had produced a 30 nm deep amorphous layer. Following implantation various anneals were carried out, including furnace annealing at 600 °C, rapid thermal annealing from 950 to 1025 °C, and spike annealing at temperatures of 1050 and 1130 °C. All anneals were performed in a N_2/O_2 5% ambient to reduce dopant loss.

Medium-energy ion scattering (MEIS) studies were carried out at CCLRC Daresbury Laboratory (Daresbury, UK) using a nominally 100 keV He^+ ion beam and the double alignment configuration, in which the channelling direction

[a]Electronic mail: J.A.Vandenberg@salford.ac.uk

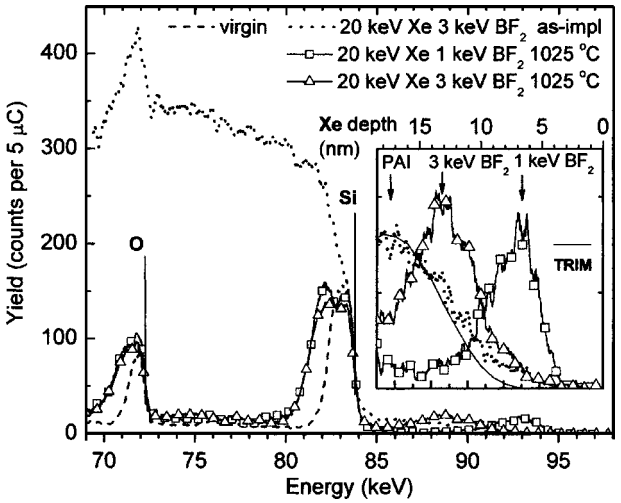

FIG. 1. MEIS energy spectra of Xe bombardment preamorphized Si samples, implanted with 1 and 3 keV BF_2^+ before and after annealing at 1025 °C for 10 s. The inset shows the depth Xe depth profiles before and after annealing.

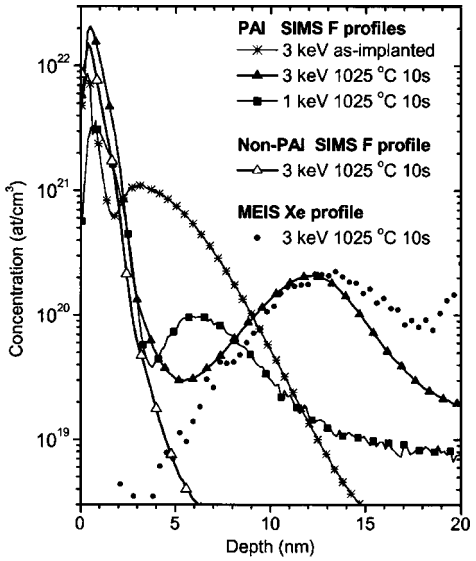

FIG. 2. SIMS F depth profiles for Xe bombardment for non- and preamorphized samples implanted with 3 keV BF_2^+ and 1 keV BF_2^+, before and after annealing at 1025 °C for 10 s. The post-annealing MEIS Xe profile for the PAI 3 keV BF_2^+ implant is also shown.

was along the $[\overline{111}]$ axis and blocking direction along [111] axis. The overall depth resolution obtained for these conditions was better than 0.8 nm.[17,18] Energy scales were converted into depth scales using established, energy dependent inelastic energy loss data.[19,20] The backscattered ion yield was calibrated by reference to the random level measured on a Si bombardment amorphized Si sample to give the implanted dose and the depth dependent concentration.

Secondary ion mass spectrometry (SIMS) analysis was performed using a Cameca Sc Ultra instrument at ITC-IRST in Trento. F depth profiles were obtained using a Cs^+ primary beam with an impact energy of 0.5 or 1 keV and an incidence angle of 45°.[21] Negative secondary ions were collected and depth scales calibrated by use of the final crater depth measured by a mechanical stylus profilometer.[22]

Energy filtered transmission electron microscopy (EFTEM) images of the Xe distribution were obtained at CNR-IMM in Catania by detecting the energy filtered image of electrons that had undergone ~670 and ~65 eV energy losses, respectively, corresponding to the Xe M and N excitation edges.

Figure 1 shows the MEIS energy spectrum of a sample processed with a Xe PAI followed by a 3 keV BF_2^+ implant as well as spectra taken after 10 s annealing at 1025 °C for both 1 and 3 keV BF_2^+ implants. The spectrum of the Xe preamorphized, 1 keV BF_2 implanted sample is identical to the 3 keV implanted one. A virgin Si sample showing scattering from the surface Si and O atoms at energies of 84 and 72 keV, respectively, is included as a reference. The increased random yield between 70 and 84 keV for the preamorphized, as-implanted sample is caused by scattering off deeper atoms in the amorphized layer. Spectra obtained after annealing show the occurrence of SPER, restoring the crystalline state. The observed increase of the width of the Si peak compared to the virgin sample is largely accounted for by the growth in oxide thickness following implantation and annealing.

The behavior of the Xe implant after annealing is the issue of interest. It is visible in the spectrum between 85 and 95 keV, and shown multiplied by a factor 10 in the inset with the Xe depth scale added. The as-implanted Xe profile extends from ~94 keV downward until it merges with the Si surface peak at approximately 85 keV. The added transport of ions in matter (TRIM) calculated Xe profile shows good agreement, giving a mean projected range (R_p) of 18 nm for 20 keV Xe. Following a 10 s anneal at 1025 °C, Xe has migrated to a shallower depth where it is trapped, producing relatively narrow distributions (4–6 nm full width at half maximum) the depths of which depend on the BF_2 implant energy. For the 1 keV BF_2 implanted sample it is at ~7 nm, and for 3 keV BF_2 at ~13 nm, as indicated by arrows. The Xe migration and trapping behavior at all other anneal conditions used, is very similar to that shown in Fig. 1, with only the samples annealed at 600 °C generally producing a somewhat broader Xe distribution.[23] The amount of retained Xe was calculated to be approximately half of the nominal 2×10^{14} cm^{-2} implanted Xe fluence. The remainder is assumed to have diffused out.

The notable observation by MEIS that the depth of the Xe accumulation depth is related to the energy of the BF_2^+ implant into the amorphous Si, suggests that Xe is trapped at a defect structure within the amorphous material caused by the BF_2 implant. However the additional possibility of a chemical interaction between Xe and F also needs to be considered. TRIM calculations show that for the low BF_2 implant energies used in this study, the B and F projectiles have similar ranges. For 3 keV BF_2^+ the mean projected range (R_p) for F is ~4.7 nm, and for 1 keV ~2.3 nm. Hence the depth of the Xe accumulation is close to $3\times R_p$, i.e., toward the end of the B and F ranges.

SIMS analysis was used for detecting F (and B) since the sensitivity of MEIS for this is relatively small. Figure 2 shows F depth profiles for preamorphized samples, as-implanted with 3 keV BF_2^+ and post annealing at 1025 °C for both 1 and 3 keV BF_2. The F depth profile for the 3 keV BF_2 nonpreamorphized sample, annealed at 1025 °C is also included. The sharp surface spike within the first 2 nm for the as-implanted sample appears to indicate a high near-surface F concentration but may also (partly) be a SIMS surface effect. For the PAI, 3 and 1 keV BF_2 implanted samples, F has migrated to the surface upon annealing, yielding a F

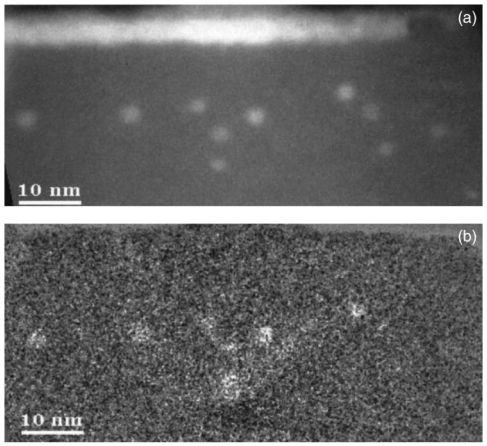

FIG. 3. EFTEM images of a Xe PAI, 3 keV BF_2 implanted Si sample after annealing to 1025 °C for 10 s using electrons with an energy loss corresponding to (a) the M ionisation edge and (b) from the N ionisation edge of Xe.

surface peak within the first 3–4 nm as clearly shown. However in both cases, there is an additional F migration into the bulk, forming second peaks at depths of 13 and 7 nm, respectively. Very similar F profiles as shown in Fig. 2 are found at these depths for all anneal conditions used, albeit that for the samples annealed at 600 °C the peaks are somewhat broader than those annealed at higher temperatures.[23] Calculation of the F retained in the second peak of Fig. 2 yields a dose of 1.35×10^{14} cm^{-2}. For all anneal conditions investigated the retained dose is between 7 and 11% of the implanted F. Note that the figure shows that for the 3 keV implanted sample without PAI, the second peak is not formed.

A detailed comparison of the post-annealing MEIS Xe depth profiles (after converting the yield to concentration) and the SIMS F profiles demonstrates the close correspondence between the two, both in shape and in concentration.[23] It is illustrated in Fig. 2 for the MEIS Xe profile for the 3 keV BeF_2 implant superimposed over the corresponding F SIMS profile The F/Xe ratio of the retained doses is ~1, although for some anneal conditions the ratio reduced to ~0.6 in particular for the 1 keV implants. Here, possibly due to their closeness to the surface, more F is lost after the high temperature anneal as shown in Fig. 2.

The possible formation of Xe agglomerates or bubbles was checked using EFTEM experiments. Figure 3(a) shows cross-sectional EFTEM images using electrons that have undergone a ~672 eV loss (M excitation edge of Xe) for a Xe PAI, 3 keV BF_2 implanted sample, annealed to 1025 °C. Any bubbles present appear as light spots, as in fact seen in the figure. To check that the spots indeed represent Xe an image using N excitation edge electrons (~65 eV loss) is shown in Fig. 3(b). It confirms the existence of Xe agglomerates at a depth between 10 and 15 nm, in agreement with the MEIS peak observed at ~13 nm for the 3 keV BF_2 implant. The size of these agglomerates was seen to grow with increasing thermal budget.

The above observations show that during SPER most F migrates to the surface, probably in front of the moving a/c interface. At the same time approximately 10% of the F moves into the bulk, to a depth corresponding to the EOR of the BF_2^+ implant. Xe equally migrates toward the surface but ~50% is trapped at the same depth while the remainder is assumed to diffuse out. It is known that defect structures can exist within an amorphous matrix, e.g., local changes in density,[16] or volume defects. The arrest of both the Xe and F at the EOR of the BF_2 implant, indicates that the accumulation effect may be related to the occurrence of such a type of defect structure. However a chemical interaction of Xe and F clearly also plays a role, since for Si preamorphized with Ge ions such an accumulation of F is not seen. The precise details of the interaction are presently not clear and further studies are in progress. It is suggested that F mediated and/or stabilized Xe agglomerates may be formed as both are known to form bubbles under certain conditions. A possible alternative to Xe agglomeration may be the formation of a XeF precipitates. In any case, the accumulated F and/or Xe at this depth and/or the damage structure that causes it, also appears to trap B during diffusion since the post anneal B SIMS profile (not shown) shows a peak with a B:F ratio of ~0.33 at the same depth.[23]

This work was supported by EU Grant No. IST-2001-32061 (IMPULSE project).

[1] X. D. Pi, C. P. Burrows, and P. G. Coleman, Phys. Rev. Lett. **90**, 155901 (2003).
[2] S. P. Jeng, T. P. Ma, R. Canteri, M. Anderle, and G. W. Rubloff, Appl. Phys. Lett. **61**, 1310 (1992).
[3] D. F. Downey, J. W. Chow, E. Ishida, and K. S. Jones, Appl. Phys. Lett. **73**, 1263 (1998).
[4] M. Y. Tsai, D. S. Day, B. D. Streetman, P. Williams, and C. A. Evans, Jr, J. Appl. Phys. **50**, 188 (1979).
[5] F. Boussaid, M. Benzohra, F. Olivie, D. Alquier, and A. Martinez Nucl. Instrum. Methods Phys. Res. B **134**, 195 (1998).
[6] M. Tamura, Y. Hiroyama, and A. Nishida. Mater. Chem. Phys. **54**, 23 (1998).
[7] A. Mokhberi, R. Kasnavi, P. B. Griffin, and J. D. Plummer, Appl. Phys. Lett. **80**, 3530 (2002).
[8] N. Ohno, T. Hara, Y. Matsunaga, M. Current, and M. Inoue, Mater. Sci. Semicond. Process. **3**, 221 (2000).
[9] C. W. Nieh and L. J. Chen, Appl. Phys. Lett. **48**, 1528 (1986).
[10] C. H. Chu and L. J. Chen, Nucl. Instrum. Methods Phys. Res. B **59/60**, 391 (1991).
[11] C. H. Chu, J. J. Yang, and L. J. Chen, Nucl. Instrum. Methods Phys. Res. B **74**, 138 (1993).
[12] G. Faraci, A. R. Pennisi, A. Terrasi, and S. Mobilio, Phys. Rev. B **38**, 13468 (1988).
[13] P. Resesz, M. Wittmer, J. Roth, and J. W. Mayer, J. Appl. Phys. **49**, 5199 (1978).
[14] M. Wittmer, J. Roth, P. Resesz, and J. W. Mayer, J. Appl. Phys. **49**, 5207 (1978).
[15] A. G. Cullis, T. E. Seidel, and R. L. Meek, J. Appl. Phys. **49**, 5188 (1978).
[16] S. Roorda, J. S. Custer, W. C. Sinke, J. M. Poate, D. C. Jacobson, A. Polman, and F. Spaepen, Nucl. Instrum. Methods Phys. Res. B **59/60**, 344 (1991).
[17] J. A. van den Berg, D. G. Armour, S Zhang and S Whelan, L. Wang, A. G. Cullis, E. H. J. Collart, R. D. Goldberg, P. Bailey, and T. C. Q. Noakes, J. Vac. Sci. Technol. B **20**, 974 (2002).
[18] M. Werner, J. A. van den Berg, D. G. Armour, W. Vandervorst, E. H. J. Collart, R. D. Goldberg, P. Bailey, and T. C. Q. Noakes. Nucl. Instrum. Methods Phys. Res. B **216**, 67 (2004).
[19] J. F. Ziegler, J. P. Biersack, and U. Littmark, *The Stopping and Range of Ions in Solids* (Pergamon Press, New York, 1985).
[20] W. K. Chu, J. W. Mayer, and M. Nicolet, *Backscattering Spectrometry*, (Academic Press, New York, 1978).
[21] M. Anderle, M. Bersani, D. Giubertoni, and P. Lazzeri, *2003 International Conference on Characterization and Metrology for ULSI Technology*, Austin, Texas, 24–28 March 2003 (AIP Conf. Proc., Vol. 683, Melville, New York, 2003), p. 695.
[22] D. Giubertoni, M. Barozzi, M. Anderle and M. Bersani, J. Vac. Sci. Technol. B **22**(1), 336 (2004).
[23] M. Werner, J. A. van den Berg, D. G. Armour, G. Carter, T. Feudel, M. Herden, M. Bersani and D. Giubertoni, P. Bailey, and T. C. Q. Noakes Mater. Sci. Eng., B **114/5**, 198 (2004).